SAND97-1842C
CONF-970968--2

Advanced micromechanisms in a multi-level polysilicon technology

M. S. Rodgers, J. J. Sniegowski, S. L. Miller, C. C. Barron, and P. J. McWhorter

Sandia National Laboratories
Mail Stop 1080
P. O. Box 5800
Albuquerque, NM 87185-1080
http://www.mdl.sandia.gov/Micromachine

RECEIVED
JUL 30 1997
OSTI

ABSTRACT

Quad-level polysilicon surface micromachining technology, comprising three mechanical levels plus an electrical interconnect layer, is giving rise to a new generation of micro-electromechanical devices and assemblies. Enhanced components can now be produced through greater flexibility in fabrication and design. New levels of design complexity that include multi-level gears, single-attempt locks, and optical elements have recently been realized. Extensive utilization of the fourth layer of polysilicon differentiates these latter generation devices from their predecessors.[1] This level of poly enables the fabrication of pin joints, linkage arms, hinges on moveable plates, and multi-level gear assemblies. The mechanical design aspects of these latest micromachines will be discussed with particular emphasis on a number of design modifications that improve the power, reliability, and smoothness of operation of the microengine.[2] The microengine is the primary actuation mechanism that is being used to drive mirrors out of plane and rotate 1600-μm diameter gears.[3] Also discussed is our most advanced micromechanical system to date, a complex proof-of-concept batch-fabricated assembly that, upon transmitting the proper electrical code to a mechanical lock, permits the operation of a micro-optical shutter.

Keywords: microengine, mirror, gear train, transmission, microactuator, polysilicon

1. INTRODUCTION

The complexity of devices that can be created using surface micromachining methods is significantly influenced by the number of mechanical layers fabricated in the process. Most components are currently limited to designs that can be defined in only two or three levels of polysilicon. The unique quad-level technology available at Sandia National Laboratories offers much greater flexibility. Consisting of three mechanical layers plus an underlying electrical interconnect, this technology permits the fabrication of actuators, gears, hubs, and the mechanical linkage arms required to interconnect these components. The microengine is a prime example of this technology, and its fabrication would not be possible with fewer layers. However, the full potential of the final polysilicon level was not initially realized due to process artifacts generated from the multi-level topography.

The implementation of chemical mechanical polishing (CMP) for planarization effectively eliminates these artifacts,[4] which show up as process stringers and mechanical interferences. Now known as the Sandia Ultra-planar Multi-level MEMS Technology (SUMMiT)[5], this process allows new levels of design complexity. Previously, the designer was constrained to defining upper level structures that were essentially isolated islands of polysilicon. Although these islands could encompass large surface areas, each had to be at least several microns from its neighbor. This made it impractical to define close-packed electrostatic elements and intermeshing gears with reasonable geometry. A significant increase in device reliability was another benefit realized through the improvements to the multi-level process technology.

Finally, the mechanical design aspects of the latest generation of multi-level micro-electromechanical sys-

Further author information -
M.S.R.: Email: rodgersm@sandia.gov; Telephone: 505-844-1784; Fax: 505-844-2991

tems (MEMS) are discussed. We start with the building blocks and conclude with a description of our most advanced system to date, a proof-of-concept single-attempt micro-mechanical lock and optical shutter combination for a safety application. This level of system complexity demands a high yield, robust actuation source. In order to enable the shutter, five out of five electrostatically controlled comb-drive assemblies[6] must function flawlessly and on the first attempt. Therefore, particular emphasis is placed on the evolution of the microengine[7] and its associated components.

2. ADVANCED POLYSILICON STACK

The technology is based on the quad-level polysilicon stack shown in figure 1.[5] Three mechanical levels of polysilicon, referred to as poly1, poly2, and poly3, are fabricated on top of a thin poly0 electrical interconnect layer. The polysilicon layers are separated by sacrificial layers of oxide that are etched away after the entire stack is fabricated. Not all layers have equal thickness. Poly0 is 0.3 µm, poly1 is 1.0 µm, poly2 is 1.5 µm, and poly3 is 2.5 µm thick. Two microns of sacrificial oxide separate poly0 from poly1 and poly2 from poly3, but only 0.5 µm separates poly1 and poly2. The differences in thickness allow for the fabrication of components with unique process requirements such as gear hubs and mirror hinges. In many areas the 0.5-µm oxide layer between poly1 and poly2 is removed during processing, so that these two levels form a single

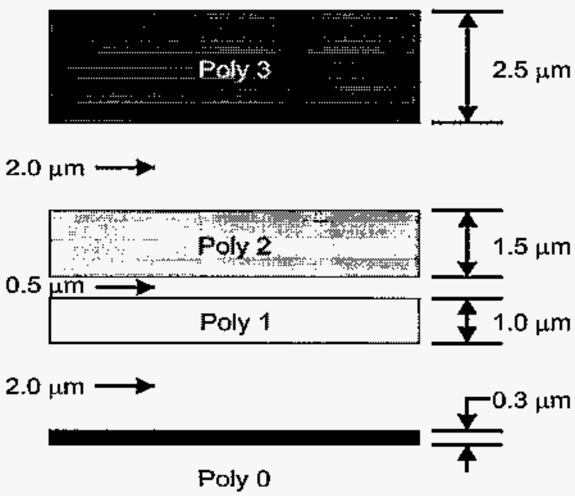

Figure 1. Sandia's four layer polysilicon / sacrificial oxide stack.

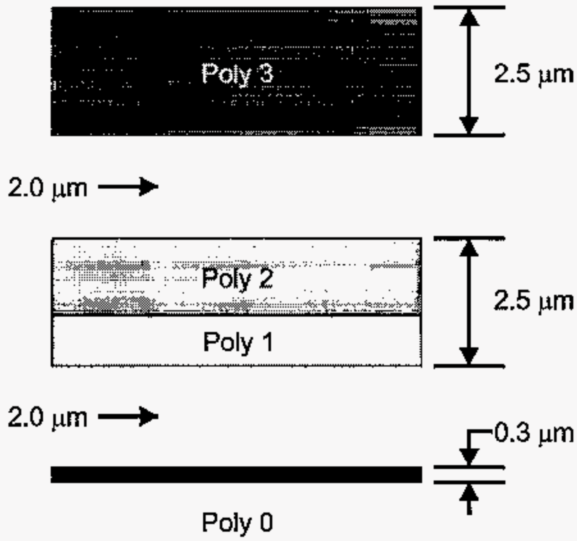

Figure 2. Where three independent layers are not required, poly1 and poly2 can be laminated to form a robust single layer.

rigid 2.5-µm thick composite layer (figure 2).

3. MICROENGINE ENHANCEMENTS

The microengine (figure 3) has evolved as one of the primary actuation mechanisms for MEMS at Sandia. It consists of two orthogonal electrostatically controlled

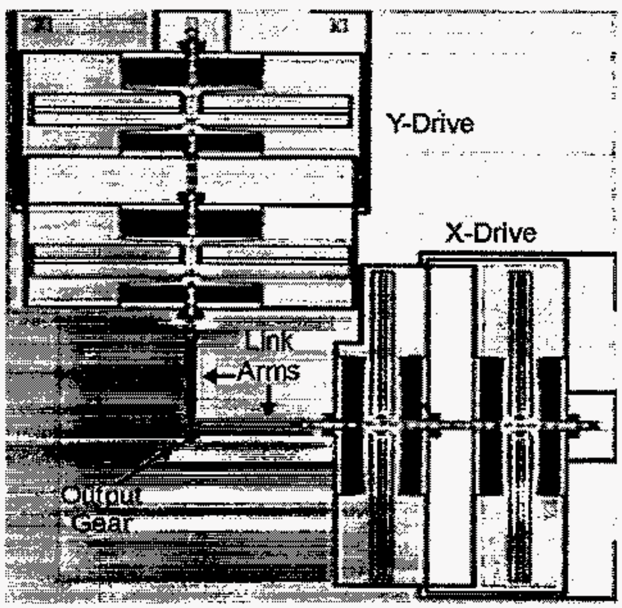

Figure 3. The microengine translates orthongonal movement from the X and Y comb drives to rotational motion of the output gear.

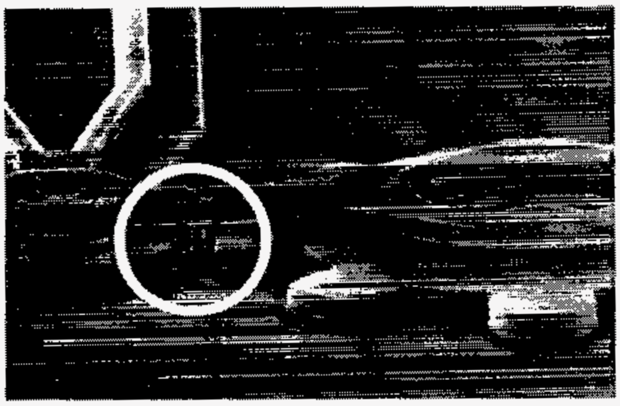

Figure 4. Undesirable film protusions such as this one introduce mechanical interference problems that limit design flexibility. The CMP planariation process eliminates these artifacts.

comb-drive assemblies, a pair of linkage arms, and an output gear. Initially developed without the CMP planarization process, the parasitic linkage arm underhang shown in figure 4 introduces a mechanical interference that requires different actuators for the "X" and "Y" drives.[2,7] The symmetrical "X" drive moves the linkage arm +/- 17 μm, while the asymmetrical "Y" drive moves +34 /–0 μm. Proper phasing of the X and Y electrical drive signals results in rotary motion of the output gear.

The first-generation comb drives were mainly defined in the 2.5 μm thick poly1/poly2 composite layer.[2] A poly0 electrical ground plane defined under the parts that move (i.e., the shuttle, support springs, wings, and attached fingers - see figure 5) is biased at 0.0 volts. The shuttle assembly is also referenced to this 0.0 volt DC potential through the electrical connections that support springs make between the shuttle and the underlying poly0. Connecting the shuttle assembly and the ground plane to the same potential eliminates the electrostatic force that might otherwise exist and that would pull the shuttle towards the substrate. Each electrostatic subassembly is comprised of four banks of fingers that operate in pairs. Banks "0" and "1" need to be simultaneously biased to pull the shuttle to the left, while a drive signal applied to the other two banks pulls the shuttle to the right.

Each bank contains 23 sets of fingers. This number was held constant while the characteristics of several finger widths and gaps were evaluated. Fingers less than 3 μm easily flexed under the 80-100 volt electrical stimulus these actuators required when driving loads. Thinner gaps between the fingers should have reduced the operating voltage or produced more force under the

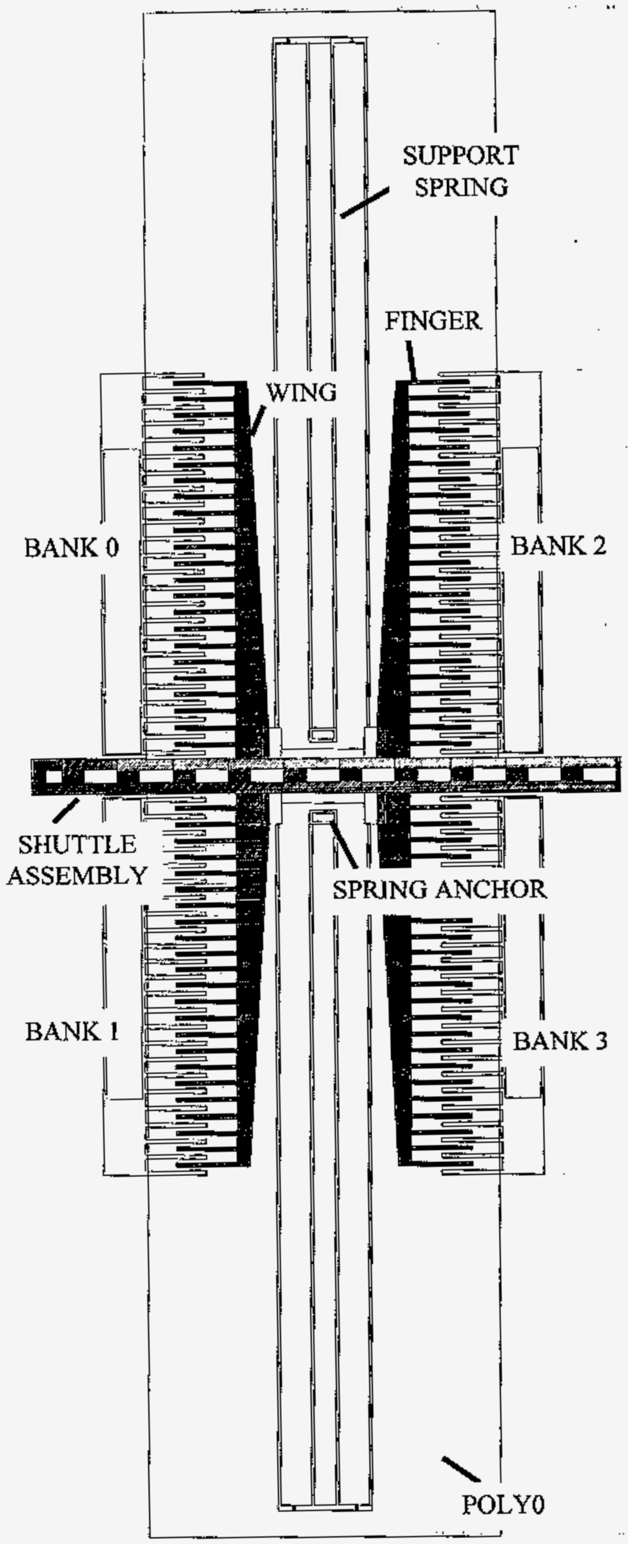

Figure 5. Each X drive in figure 3 uses two of these electrostatic subassemblies. The fingers and springs are offset 17 μm in the Y drive to allow for its asymmetrical travel.

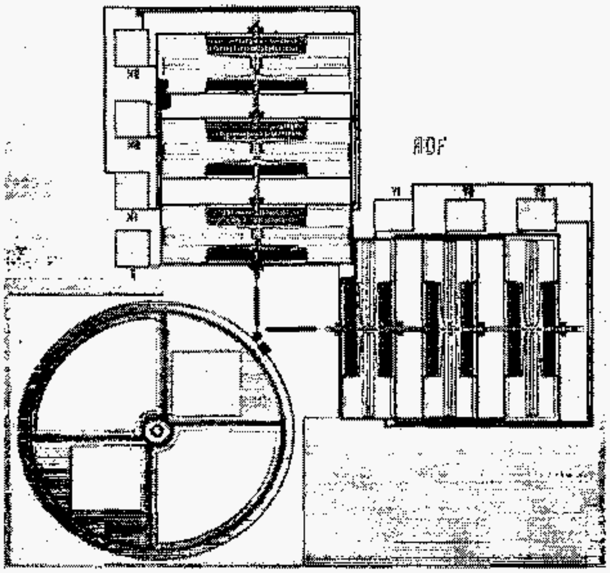

Figure 6. Triple electrostatic subassemblies in each comb-drive generate sufficient force to rotate this 1600-μm diameter optical shutter.

same conditions. However, slight asymmetries in the fabricated device and small but significant off-axis forces that occur during microengine operation actually made the flexing problem worse. This forced the use of wider gaps. The evaluation resulted in the established use of 3-μm gaps and 3-μm wide fingers.

In a different approach, several electrostatic subassemblies were cascaded in series to generate more force. This proved to be much more reliable than trying to reduce finger gap. This approach was used to successfully drive the first generation 1600-μm optical shutter shown in figure 6.[3] In this case each comb drive employs three electrostatic subassemblies. A major disadvantage of cascading is that it is chip area consumptive, and therefore costly to implement. One version of the optical shutter used comb drives composed of two electrostatic subassemblies. Although functional, it proved to be much less dependable than its triple counterpart.

Another aspect of the operation of a comb drive as a linear actuator is the astable nature of the lateral position of the fingers.[1] These comb drives depend on folded beam support springs to keep the moveable fingers centered between the fixed ones. If the fingers remain precisely centered, then the lateral electrostatic forces exactly cancel. In operation, however, once the fingers are displaced to one side or the other, an instability begins. The side with the smaller gap produces the greater force on the fingers which, in turn,

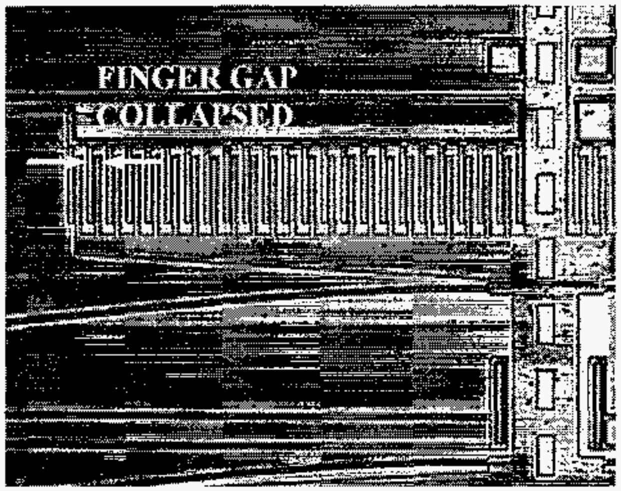

Figure 7. Too high of an electrical drive signal causes the shuttle assembly to laterally clamp against the stationary fingers.

tends to collapse the gap even further. Eventually this will overcome the restoring force of the support springs, and the finger gap will collapse and clamp as shown in figure 7.

One solution to this problem is to fabricate mechanical stops on each side of the shuttle to limit lateral travel. However, current photolithographic restrictions dictate a design rule that elements on the same layer must be separated by at least one μm. Although normally adequate, a 1.0-μm gap between the shuttle and a lateral travel limiter is too wide to be useful. Fortunately, this restriction applies only to the as-fabricated position. Released parts can engage each other with much tighter fits. The lateral alignment guides shown at the end of the comb drive in figure 8 meet the

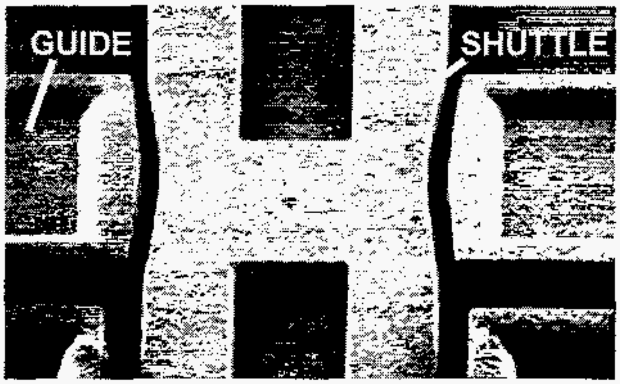

Figure 8. These lateral guides limit horizontal movement of the shuttle to 0.5 μm once the shuttle slides up towards top of photo. Other guides have been fabricated that constrain lateral displacement to within 0.25 μm.

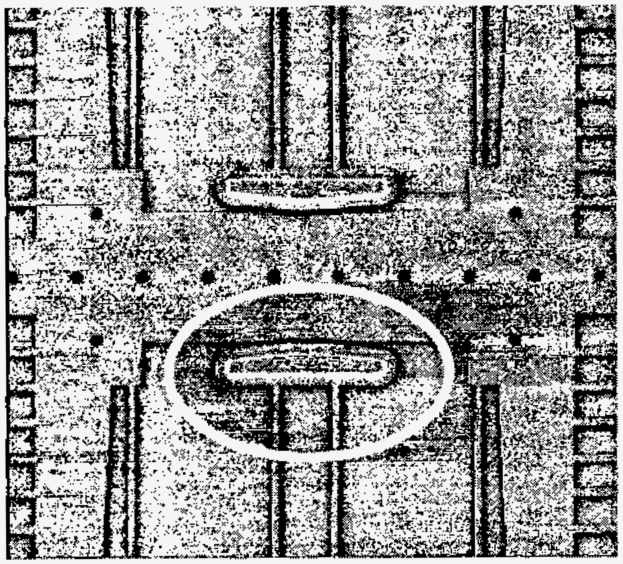

Figure 9. Incorporating the lateral guides into the support spring anchors helps conserve valuable die area.

1.0–μm gap requirement, yet constrain the shuttle to 0.5 μm lateral movements during operation. This modification permits the replacement of the triple drives with the dual drives by allowing the use of higher operating voltages without the associated clamping.

Further die area was saved by moving the two remaining subassemblies closer together and incorporating the travel limiters into the support spring anchors as shown in figure 9. At this point the overall width of the comb drive is dictated by the length of the folded beam support springs. Each spring is 500 μm long, which yields an overall comb-drive width of just over 1 mm. Since the force required to displace the spring varies as the cube of its length,[8] shortening the springs would save little in terms of real estate yet significantly increase the voltage required for operation. Lengthening the springs to reduce the voltage requirements is also unattractive since the springs already tend to drag on the surface and inhibit operation.

The modifications discussed thus far have been defined in the poly1/poly2 composite layer. We now discuss utilization of poly3. Since the force produced by electrostatic elements is proportional to the thickness of its fingers,[8] fabricating a second layer of fingers in poly3 over the existing poly1/poly2 fingers promised a doubling of the drive force without additional real estate requirements. Attempts before CMP planarization[4] resulted in the formation of a stringer (figure 10) around each finger that prevented operation. The CMP process successfully eliminated these stringers, and the expected force doubling was realized. However, lateral clamping once again became an issue. In this case, the main shuttle body was distorting under the additional force generated. Reinforcing the shuttle with a corrugated section of poly3 solved this problem.

Poly3 was also employed to significantly increase the out-of-plane or "Z" axis stiffness for both the support springs and moveable shuttle assembly. This was accomplished by fabricating a second folded beam support spring over the standard poly1/poly2 suspension and anchoring the two together every 100 μm. Reliability improved tremendously due to the increased "Z" stiffness which eliminated dragging and sticking of the support springs to the underlying substrate. Total "Z" stiffness increased approximately a factor of twenty as this parameter is proportional to the cube of the thickness. However, the stiffness along the desired line of motion only increased by a factor of 2, which was automatically compensated by the additional poly3 layer of fingers.

One final comb-drive issue was also addressed. When the "Y" drive was displaced the full 34 μm the support springs could buckle and introduce erratic comb-drive operation. To cure this, multi-level stops that prevented excessive travel were added near the ends of the support springs (figure 11). These worked well and were added to all of the springs as a precautionary measure. The final product is a robust and reliable actuator that provides more than twice the output force of its predecessor while requiring only 2/3 the die area.[1]

Figure 10. Prior to CMP, hundreds of poly3 stringers like the ones shown above formed around the comb drive fingers preventing operation. Stringers in photo fell to the underlying poly0 after the final release etch.

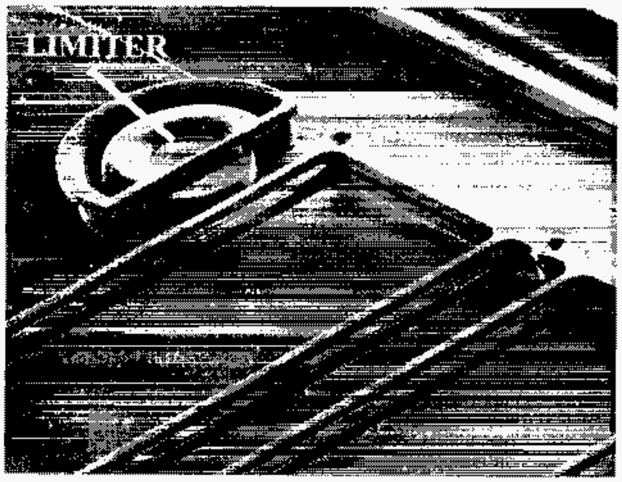

Figure 11. Multi-level support springs and travel limiters significantly increase comb-drive robustness and reliability.

3. MICROENGINE APPLICATIONS

One fundamental requirement for the microengine is the ability to drive another gear or a set of gears. This capability was first demonstrated by Sniegowski and Garcia[7,9] when early microengines were used to drive a 1600-μm optical shutter and a group of five 50-μm gears in a straight-line configuration. These were very successful achievements, even though properly designed gear teeth were difficult to implement at the time due to limitations imposed by the layout tools. Binding problems with the gears made slow speed and start/stop operation problematic.[1] Current gear teeth are generated with an in-house software program that defines an almost perfect involute profile for each gear

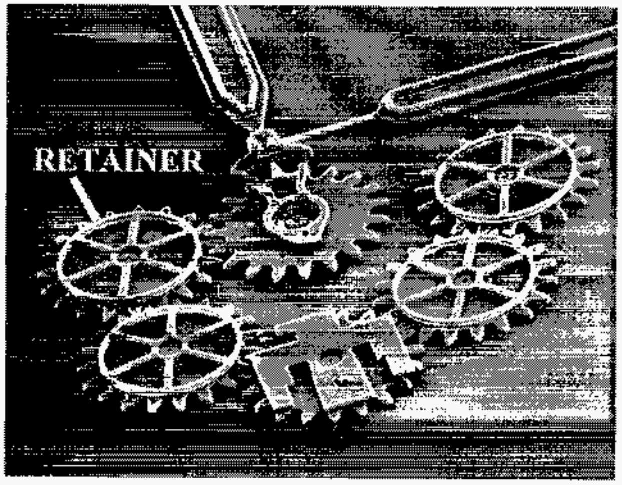

Figure 12. The company logo and circular rings assure precise alignment of this high speed cluster. Each 19 tooth gear is 76 μm in diameter.

tooth.[10] In addition, stationary poly3 retainers with dimples were fabricated on top of the gears to limit "Z" axis travel and insure precise vertical alignment. Together these changes result in very smooth gear action, highly reliable start/stop performance, and enhanced high-speed operation. The six-gear cluster in figure 12

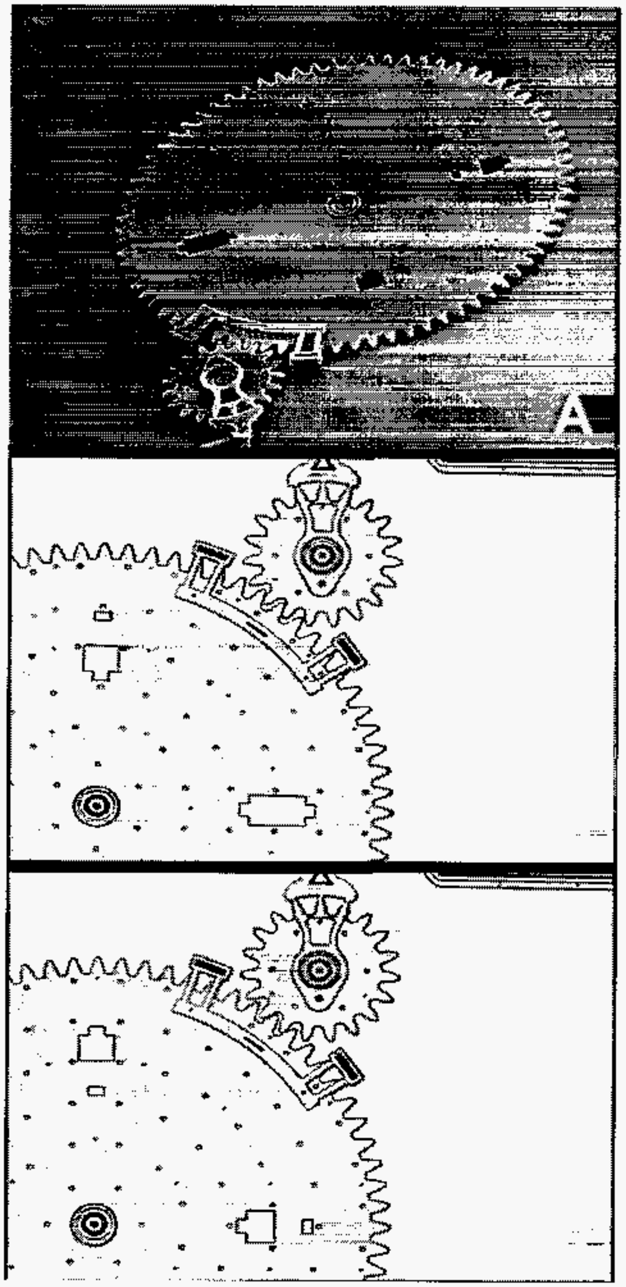

Figure 13. This 2-bit coded wheel changes its bit pattern each time the smaller microengine drive gear rotates one full revolution. The microengine is stable in this position. Thus the code can be retained indefinitely even with power removed.

incorporates the latest features and has been operated at over 250,000 rpm.

Another attribute associated with the microengine is its tendency to return to and remain in its fabrication position when electrical power is removed. This is due to the restoring force of the comb-drive support springs, and it is beneficial for applications that can make use of single or an integer number of micro-engine output gear revolutions. The 2-bit coded wheel in figure 13 is an excellent example. Each complete revolution of the microengine drive gear or pinion rotates the wheel 90 degrees. Optical interrogation of the wheel can then be used to determine the wheel state or current position.

Even though the microengine produces rotary motion, it can still be used for many applications requiring long linear throws. Comb drives provide linear motion, but practical implementations limit travel to a few tens of microns. Figure 14 is a SEM image of a microengine driven rack and pinion assembly that has a total throw just under 1 mm. Here poly3 is utilized to create an open housing that constrains rack movement yet permits the rack to be connected to external conponents.

Two approaches were pursued to create self-assembling pop-up mirrors that could be used to deflect laser beams. Both required the use of long throw linear racks. Dual microengines with a dual-sided rack assembly are used to generate the necessary force in one design. The other uses a single microengine with a micro-transmission[1] coupled to a single-sided rack assembly to accomplish the same task (figure 15). This

Figure 14. Close-up of rack and pinion engagement. The rack is confined within a housing defined in poly3. Note the involute teeth on the drive gear.

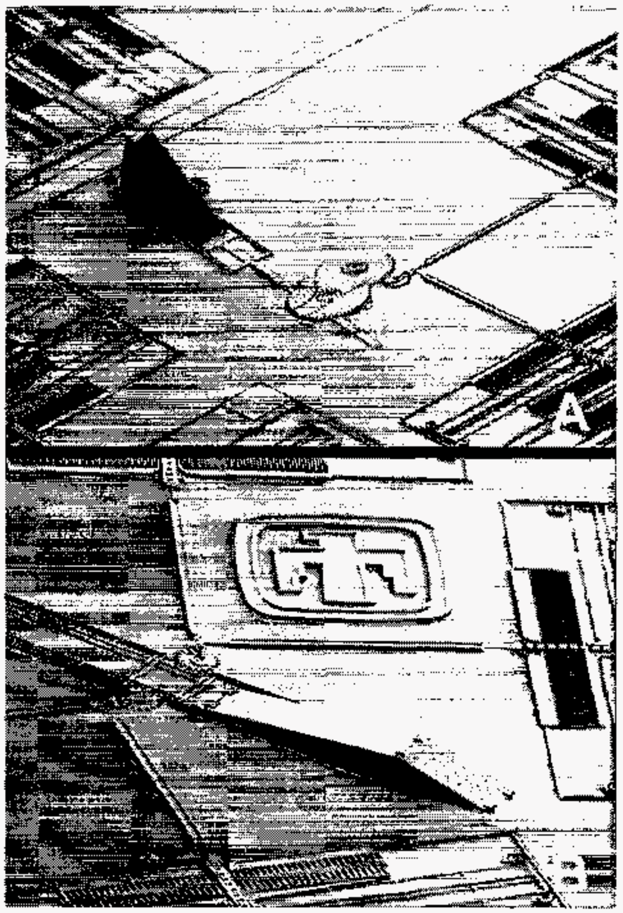

Figure 15. The single microengine and transmission combination (A) produces more force and consumes less area than the dual microengine pop-up mirror (B).

transmission is comprised of two compound or dual-level gears. Each gear has a lower set of teeth fabricated in the composite poly1/poly2 level and an upper set fabricated in poly3. Poly3 is also used in the fabrication of the hinges interconnecting the mirror plates (figure 16) and the mirror track guide rails. The transmission driven unit has significant advantages over the dual microengine approach. It requires half the real estate, has fewer electrical interconnects, and can generate about five times as much force on the rack as the two microengines combined. Furthermore, additional gears can be incorporated into the transmission to produce even more force. Gear reduction units impose a speed penalty, but in most cases the high rpm capability of the microengine make this point irrelevant.

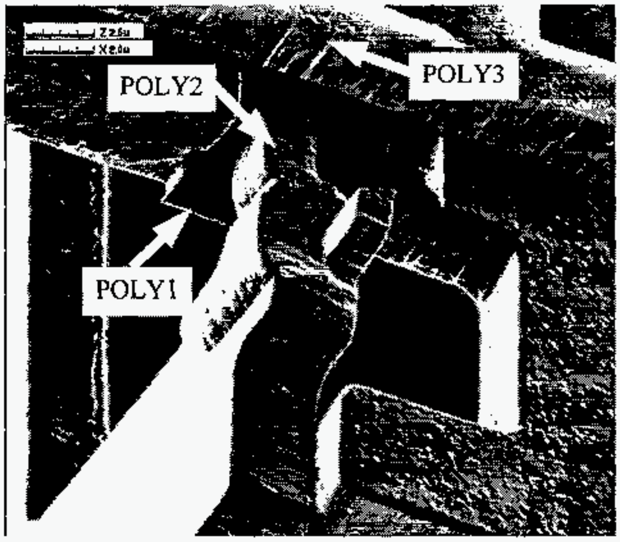

Figure 16. Close-up of hinge connecting the mirror plates. Note that all three mechanical layers of polysilicon are easily decernable.

4. COMBINED FUNCTIONS

Many safety and security systems could make use of MEMS to enhance their effectiveness. Several mechanical locks based upon a pin-in-maze[11] concept were fabricated in support of such applications. The basic design for these structures is shown in figure 17. A standard microengine rotates the wheel into which the maze is "cut", while a third comb drive directly manipulates an arm that overlaps the wheel and supports a pin riding within the maze track. Navigation of the pin through the maze requires a series of steps in which the arm is energized to position the pin radially, and then the drive gear is rotated to bring the maze to the next decision point.[5] This is a single-attempt device. Once a wrong decision is made, the pin follows a maze path that terminates in a locked position. An anti-reverse spring prevents reverse operation, so the decision cannot be retried.

Although the pin-in-maze lock performs the mechanical discrimination function, to be useful some other component must be enabled when, and only when, the lock receives the correct signal sequence. To demonstrate this capability an enhanced pin-in-maze microlock has been integrated with a 1600-µm diameter shutter assembly (figure 18F) that needs to be rotated 90 degrees clockwise to allow optical signal passage. With an overall width of 3800 µm and length of 4730 µm, this totally batch-fabricated system is large compared to most surface micromachined assemblies. One design requirement states that the shutter opening needs to be big enough to accommodate integration with current vertical cavity surface emitting laser (VCSEL) and optical fiber technologies. In absolute terms this means a 400-µm diameter opening, a feature size readily supported by and the reason for developing the 1600-µm shutter.

The optical shutter microengine is fabricated with a mechanical pin that functions like a deadbolt mechanism (figure 18A) to prevent linkage arm movement. This makes it impossible to operate until the pin, held in its fabricated locked position by a dual spring clamp (figure 18E), is pulled by an arm interconnected to the micromechanical lock. This arm spans the two circled regions shown in figure 18F, and its ends are detailed in figures 18E and H. In addition to the springs, the arm is held in place at both ends and in the middle with poly3 retainers. Also, just in from the retainers at both ends and twice along its length, poly3 wings are attached to the arm. These help prevent the arm from twisting and further enhance reliability by reducing the surface contact area.

The pin-in-maze lock assembly is of the same basic design discussed earlier. However, the maze hub diameter was significantly increased (figure 18D), and a poly3 retainer has been constructed around the microengine drive gear (figure 18H). Both of these features provide much greater out-of-plane control to insure that parts remain vertically aligned. The comb drive and maze pin arm shown in 18C remain unchanged, but the pin itself (figure 18B) is the design that proved to be the most reliable of three configurations evaluated.

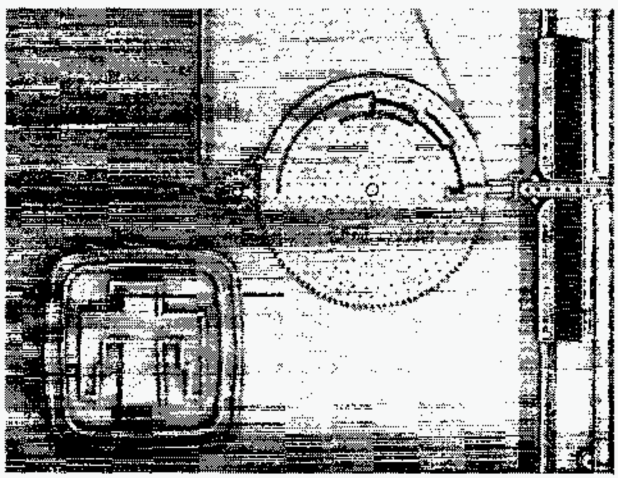

Figure 17. Prototype three decision point pin-in-maze assembly uses a microengine to rotate the maze wheel, while a comb-drive actuator controls pin position.

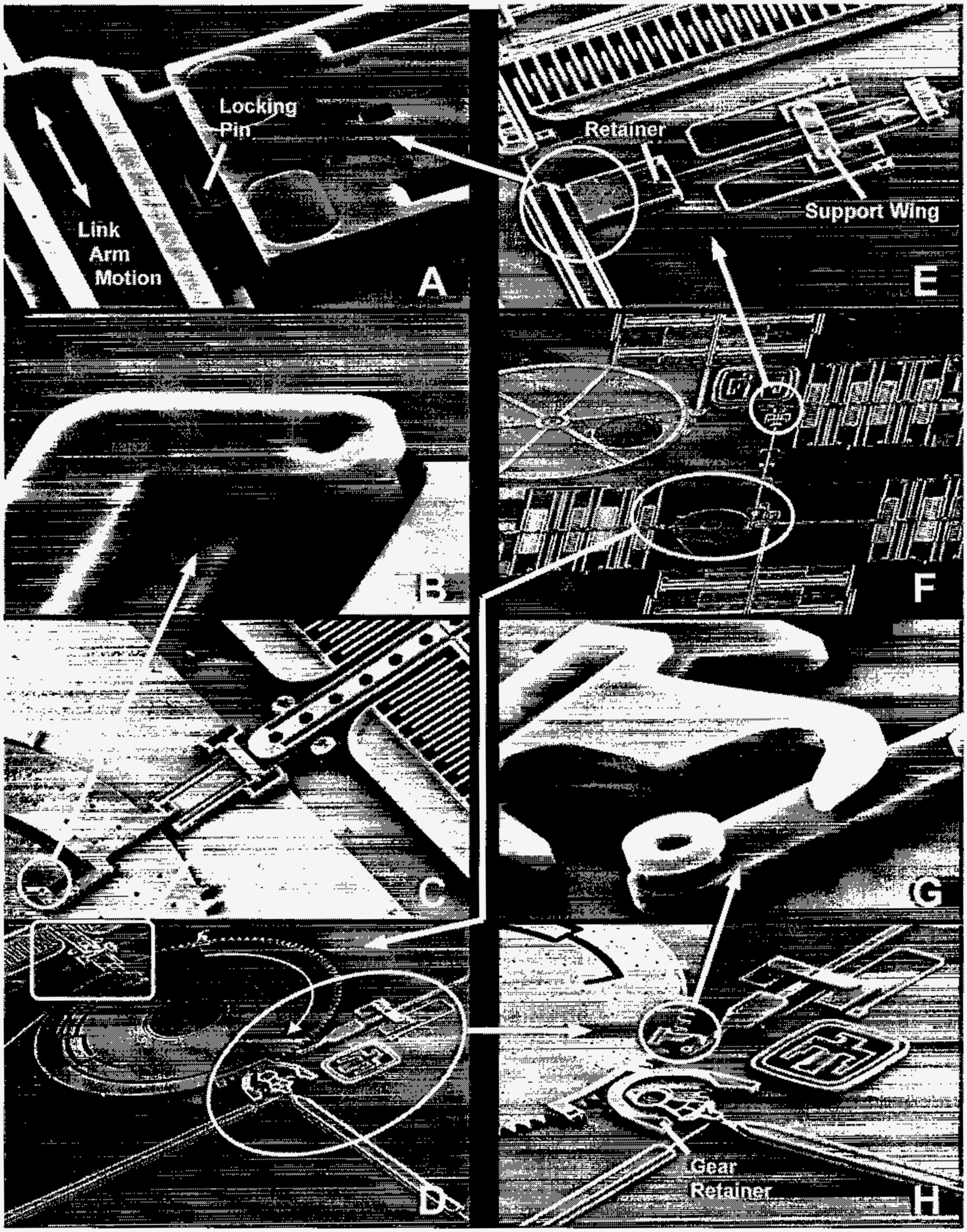

Figure 18. Micromechanical lock and shutter assembly. Overview shot is given in figure F. Note that a section of the shutter and parts of the comb drives are cut off in image. All other shots are close-ups of the indicated regions.

Note the poly3 hook on the maze wheel at the top of figure 18D. As the maze is negotiated, this hook rotates clockwise. If all decisions are correctly made the hook eventually engages a poly3 pin attached to the top of the deadbolt linkage arm (figures 18G & H). Another partial turn of the pin-in-maze drive gear pulls the deadbolt out of the microengine linkage arm that drives the optical shutter. The second microengine then drives the shutter to the enabled position, and the optical signal path is complete. The entire operation occurs in less than 100 milliseconds. Successful operation of this device with a VCSEL mounted to the backside of the wafer has also been demonstrated.

The primary goal of this assemblage was to demonstrate that the necessary level of complex interactions can be realized with surface micromachined technology. Although this combined set of functions does not possess the details of a fieldable mechanical lock, it successfully demonstrates that full-up devices will be possible.

5. SUMMARY

The first operational microengines demonstrated that a quad-level polysilicon technology offers tremendous potential. Through a continuous sequence of design improvements, many enabled by advances in fabrication technology, we have begun to exploit that potential. For example, our latest comb drives produce many times the force per unit area of their predecessors. Furthermore, this force can be multiplied by orders of magnitude with newly developed microtransmissions. For years engineers were constrained to designing modest assemblies that could be powered by a few micronewtons of force. Now we can work with hundreds of micronewtons, and in the near future it is conceivable that actuation systems capable of delivering millinewtons or even tens of millinewtons will be available. Forces at this level are sufficient to fabricate large self-assembling 3D structures with functionality not yet conceived.

For the present we are creating complex assemblies that perform useful functions and with significant benefits when compared to macro components. These benefits are primarily size, mass, self-assembly, and batch fabrication. In its present form the micromechanical lock only has application as a research prototype, and a demonstration of the technology. However, its success and the success of the other structures discussed here are being combined to produce a system that dramatically surpasses the current device. In fabrication are systems that would have been hard to imagine just a year ago, and the current development pace shows no signs of slowing.

ACKNOWLEDGEMENTS

The authors are grateful to Michael Callahan for funding this work, and the personnel of the Microelectronics Development Laboratory at Sandia National Laboratories for fabricating and evaluating the devices used in this study.

Sandia is a multiprogram laboratory operated by Sandia Corporation, a Lockheed Martin Company, for the United States Department of Energy under Contract DE-AC04-94AL85000.

REFERENCES

1. J. J. Sniegowski, S. L. Miller, G. LaVigne, M. S. Rodgers, and P. J. McWhorter, "Monolithic Geared Mechanisms Driven by a Polysilicon Surface Machined On-chip Electrostatic Engine", *Technical Digest of the 1996 Solid State Sensor and Actuator Workshop*, Hilton Head Island, SC, pp.178-182, June 3-6, 1996.

2. J. J. Sniegowski and E. J. Garcia, "Microfabricated Actuators and Their Application to Optics", *Proc. SPIE Miniaturized Systems with Micro-Optics and Micromechanics, 2383*, 2/7-9/95, San Jose, CA, pp. 46-64, 1995.

3. E. J. Garcia and J. J. Sniegowski, "Surface Micromachined Microengine as the Driver for Micromechanical Gears", *Proc. of the 8th International Conf. on Solid-State Sensors and Actuators and Eurosensors IX,* 6/25-29/95, Stockholm, Sweden 1, pp. 365-368, 1995.

4. R. D. Nasby, J. J. Sniegowski, J. H. Smith, S. Montague, C. C. Barron, W. P. Eaton, P. J. McWhorter, D. L. Hetherington, C. A. Apblett, and J. G. Fleming, "Application of Chemical-Mechanical Polishing to Planarization of Surface Micromachined Devices", *Technical Digest of the 1996 Solid State Sensor and Actuator Workshop,* Hilton Head Island, SC, pp.48-53, June 3-6, 1996.

5. More technical information can be found at the web site http://www.mdl.sandia.gov/Micromachine.

6. W. C. Tang, T-C. H. Nguyen, and R. T. Howe, "Laterally Driven Polysilicon Resonant Microstructures," *Sensors and Actuators, 20*, p. 25, 1989.

7. E. J. Garcia and J. J. Sniegowski, "Surface Micromachined Microengine", *Sensors and Actuators A, 48*, p. 203, 1995.

8. W. C. Tang, Ph.D. Thesis, University of California, Berkeley, 1990.

9. J. J. Sniegowski and E. J. Garcia, "Surface Micromachined Gear Trains Driven by an On-Chip Electrostatic Microengine", IEEE Electron Device Letters, Vol. 17, p. 366, July 1996.

10. H. E. Merrit, *Gear Engineering*, Chps. 4 and 6, Pitman Publishing, 1971.

11. G. L. Benavides, "Rotary Pin-In-Maze Discriminator", U. S. Patent 5626040, Sandia National Laboratories, May 6, 1997.